

Physics-Informed Channel Modeling with Ultrasound Localization Microscopy: Reconstructing Geometry and Flow Field from Sparse Velocity Measurements

Luca Giaccone

Dept. of Information Engineering
and Computer Science
University of Trento
Trento, Italy
0009-0001-8432-367X

Giulia Tuccio

Dept. of Information Engineering
and Computer Science
University of Trento
Trento, Italy
0000-0001-5419-5892

Libertario Demi

Dept. of Information Engineering
and Computer Science
University of Trento
Trento, Italy
0000-0002-0635-2133

Abstract—Ultrasound localization microscopy (ULM) has improved microvascular imaging by tracking microbubble (MB) trajectories to reconstruct vessel networks. However, the ensemble of trajectories produced by this technique is usually difficult to interpret, due to the underlying complexity of vascular geometries, MB motion, and unavoidable localization and tracking errors. In this work, we introduce a physics-informed channel modeling approach that reconstructs both vessel geometry and flow field exclusively from MB velocity measurements. By leveraging the inherent flow dynamics, each MB refines the vessel model, thus creating a unique, physically coherent reconstruction. We validate our method on an *in vitro* dataset, showing its robustness under sparse measurement conditions. This approach might allow for recovery of vessel information in tubes with low track density, while facilitating the extraction of clinically relevant global features.

Index Terms—Ultrasound localization microscopy, channel reconstruction, sparse measurements

I. INTRODUCTION

Over the past decade, ultrasound localization microscopy has made significant progress, achieving the reconstruction of vascular networks at sub-wavelength resolution [1]–[5]. Despite these advances, ULM still faces several challenges that limit its clinical applicability. One key issue is the trade-off between acquisition time and vessel saturation [6]–[8]. Increasing MB concentration can accelerate vascular perfusion, but it often leads to poor detection and tracking performance. Furthermore, ULM measurements are complex and highly susceptible to noise, as a large number of MBs must be accurately detected, localized, and tracked across many frames. Errors can propagate through each stage of the processing pipeline, leading to outcomes that are difficult to use for quantitative vascular analysis or clinical assessments.

In this study, we propose a physics-informed method for channel modeling from ULM velocity data. By incorporating physical priors and constraints, the method enables robust reconstruction even from sparse MB measurements. Rather

than directly relying on clouds of individual MB tracks, our approach extracts a coherent representation of the vascular geometry and flow profile. This representation has the potential to improve interpretability and usability of ULM outputs. It simplifies the complex raw data into meaningful information, facilitating further analysis and the identification of macroscopic vascular biomarkers useful for clinical applications.

II. METHODS

A. Data acquisition and ULM velocity measurements

We performed an *in vitro* experiment to study flow through a tube with variable radius (see Fig. 1a). Ultrasound data were acquired using a linear array probe connected to the ULAOP research platform, operating at a framerate of 46.5 Hz. Across multiple acquisitions, we collected more than 5000 MB trajectories. MBs were tracked using the Hungarian algorithm, obtaining the velocities displayed in Figure 1b. In total, we measured over 55000 MB velocities. The tube was built by linking two cylindrical channels with different radius. The result is a pipe featuring two distinct sections: a narrow upstream segment with dense MB saturation and a wider downstream segment with sparser MB detections. This variability introduced heterogeneity in the data, allowing to assess the reconstruction performance across diverse conditions. The tube's centerline was manually segmented to assign a radial coordinate r to each MB measurement. We thus analyzed the set of velocity measurements $\{u(r, x)\}$, where x is the axial coordinate along the tube.

B. Channel Modeling

We divided the tube into overlapping windows along the x -axis (see Fig. 1b). Within each window, we fitted a Poiseuille flow model to the local velocity measurements $\{u(r, x)\}$, obtaining estimates of the maximum velocity \hat{u}_{\max} and the radius \tilde{r} . We also recorded the mean square error (MSE) of

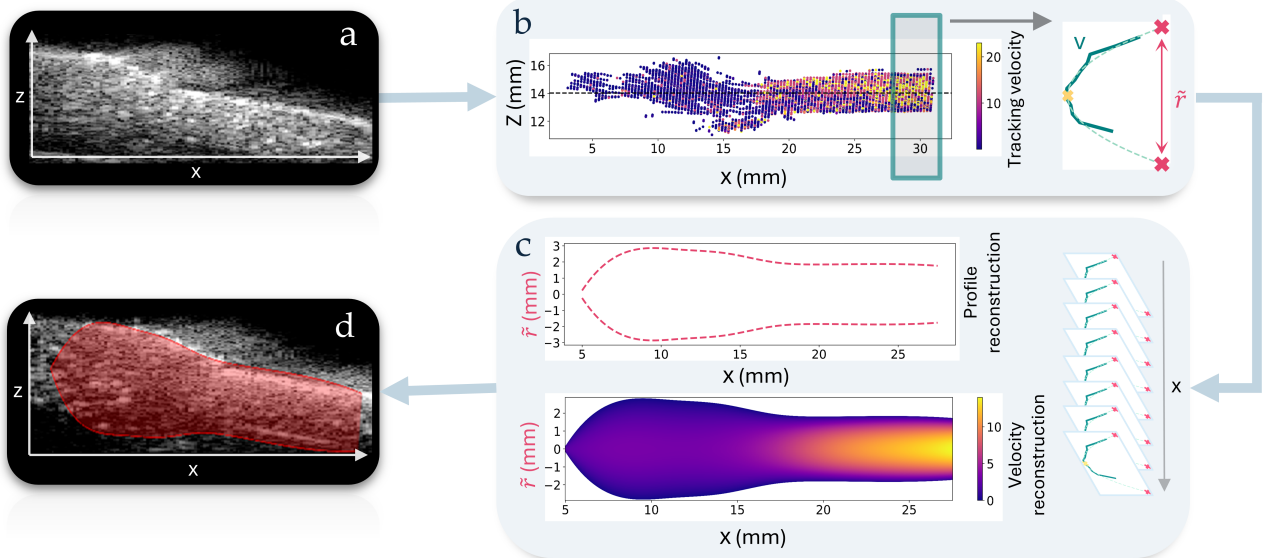


Fig. 1. Channel reconstruction pipeline: (a) maximum intensity projection (MIP) of the acquired B-mode dataset, (b) MB velocities estimated from ULM, with illustration of the local Poiseuille fit within a sliding window, (c) radial profile and velocity field reconstruction obtained through local estimates interpolation, (d) reconstructed tube geometry compared to the MIP image.

the model fitting to quantify local deviations from the ideal profile.

To reconstruct a global representation of the channel, we interpolated the local estimates to obtain smooth profiles of the radius $R(x)$ and the maximum velocity $u_{\max}(x)$ (see Fig. 1c). Before the interpolation, we discarded windows where the estimated radius exceeded twice the maximum observed radius in that window, which was indicative of poor or invalid fits. The remaining data points were then interpolated using a MSE-weighted smoothing spline. Specifically, the spline interpolation was formulated as the minimization of the following cost functional

$$J = \sum_i w_i (f(x_i) - y_i)^2 + \lambda \int \left(\frac{\partial^2 f(x)}{\partial x^2} \right)^2 dx \quad (1)$$

where y_i are the local radius or velocity estimates, x_i the corresponding axial positions, $f(x)$ is the radial or maximum velocity profile to compute, $w_i = 1/(1 + MSE_i)$ are weights derived from the mean square errors MSE_i of the Poiseuille fits at the i -th window, and λ is a regularization parameter controlling the smoothness of the interpolation. In all experiments, we set $\lambda = 0.1$.

This approach is particularly effective when using small windows with high overlap, where many densely sampled local fits are available. In such cases, a moderate amount of smoothing helps to ensure that the reconstructed channel profile remains both stable and physically plausible. In this study, we used a window size of 2 mm and a step size of 0.2 mm between adjacent windows. Nonetheless, we observed that the reconstructed profiles remained stable even when these parameters were varied within reasonable bounds.

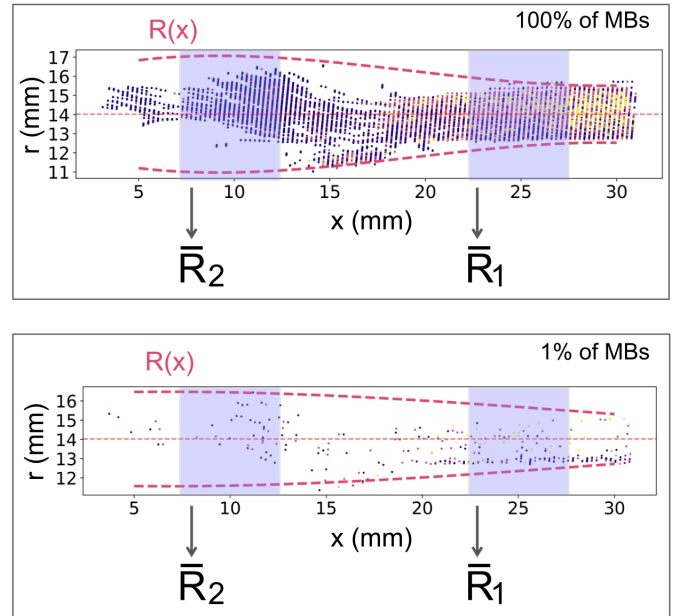


Fig. 2. Representative radial profile reconstructions using 100% and 1% of the available dataset. The violet areas highlight the two intervals, $I_1 = [7.5, 12.5]$ and $I_2 = [22.5, 27.5]$, over which the radial profiles were averaged to estimate the vessel radius in the two tube sections.

C. Evaluation of radii estimation

We evaluated the robustness of the reconstruction under varying data availability. To this end, we sampled a fraction p , with $p \in [0.01, 1]$, of the available velocity measurements and performed the reconstruction based on the reduced dataset. As shown in Fig. 2, we then computed the average estimated

radii \bar{R}_1 and \bar{R}_2 in the upstream and downstream sections, respectively. These estimates were obtained by averaging the reconstructed radius profile $R(x)$ over two axial intervals where the true radius was known to be constant (i.e., sufficiently far from the transition region between the two segments). To ensure statistical robustness, we repeated the random sampling procedure 100 times for each value of p , and averaged the resulting estimates.

III. RESULTS

As shown in Fig. 1, the reconstructed tube geometry closely approximates the original shape. The two distinct sections are well captured, and the transition region between them appears smooth and continuous. The reconstructed velocity field also reflects the expected flow behavior: a higher velocity within the narrow section and a decrease in the wider segment. In addition, the method effectively removes spurious peaks in the velocity profile, which are likely due to tracking errors or measurement noise, resulting in a smooth and coherent representation.

Figure 3 presents the outcome of the radius estimation analysis described in Sec. II-C. The true radii $R_1 = 1.6 \text{ mm}$ and $R_2 = 3 \text{ mm}$ are known by design. The plot shows how the estimated radii vary with different sampling percentages of the available velocity data. For each sampling level, the mean radius values are reported as solid lines, while the corresponding standard deviations are indicated by shaded regions.

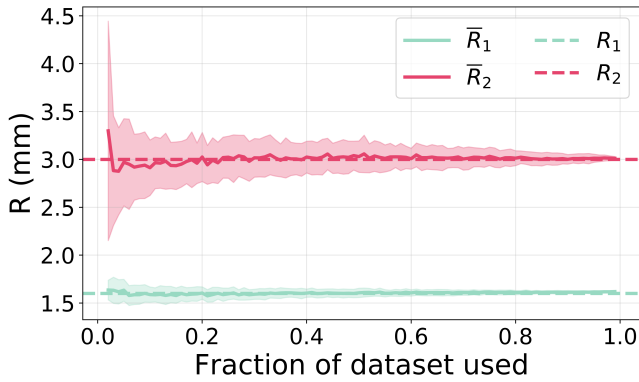


Fig. 3. Behavior of the radial estimates \bar{R}_1 and \bar{R}_2 as a function of the available dataset fraction. The true radii R_1 and R_2 are shown as dashed lines for reference.

IV. DISCUSSION AND CONCLUSIONS

Figure 3 provides positive evidence that robust reconstruction is achievable even in sparse MB scenarios. Notably, the estimated radius \bar{R}_1 closely approximates the true value with remarkably low variance, even when using as little as 1% of the available data. On the other hand, \bar{R}_2 exhibits higher variability as we decrease the available dataset, but the result remains quite accurate considering the raw measured data in this segment, which are more sparse and less informative. Moreover, tube enlargement may induce flow turbulence,

further disturbing the measurements. Turbulent flow introduces complexity beyond the simple assumptions of the Poiseuille model, potentially limiting the effectiveness of the proposed reconstruction approach. However, in smaller vessels, where ULM is most relevant, the Reynolds number is lower, and laminar flow dominates. In this regime, velocity measurements are more reliable, further reinforcing the suitability of this approach for microvascular applications.

The proposed reconstruction method offers two key advantages. First, it enables the extraction of meaningful information from noisy data by integrating multiple local perspectives: informative measurements are emphasized, while unreliable or inconsistent data are naturally down-weighted through MSE-based weighting and outlier rejection. Second, the use of a smoothing spline introduces spatial regularity, allowing neighboring estimates to jointly influence the final profile. This reduces the impact of local fitting errors, prevents overfitting to isolated deviations, and results in a more coherent and stable reconstruction.

Future work will focus on refining the methodology to improve robustness while studying the extraction of macroscopic tube features, such as the pressure profile at tube boundaries, which may hold clinical relevance. In particular, we aim to extend the approach to *in vivo* datasets, where additional challenges must be addressed.

REFERENCES

- [1] Song P, Rubin JM, Lowerison MR. Super-resolution ultrasound microvascular imaging: Is it ready for clinical use? *Z Med Phys.* 2023 Aug.
- [2] Dencks S, Lowerison M, Hansen-Shearer J, Shin Y, Schmitz G, Song P, Tang MX. Super-Resolution Ultrasound: From Data Acquisition and Motion Correction to Localization, Tracking, and Evaluation. *IEEE Trans Ultrason Ferroelectr Freq Control.* 2025 Apr.
- [3] Errico, C., Pierre, J., Pezet, S. et al. Ultrafast ultrasound localization microscopy for deep super-resolution vascular imaging. *Nature* 527, 499–502 (2015).
- [4] O. Couture, V. Hingot, B. Heiles, P. Muleki-Seya and M. Tanter, "Ultrasound Localization Microscopy and Super-Resolution: A State of the Art," in IEEE Transactions on Ultrasonics, Ferroelectrics, and Frequency Control, vol. 65, no. 8, pp. 1304-1320, Aug. 2018.
- [5] Yi HM, Lowerison MR, Song PF, Zhang W. A Review of Clinical Applications for Super-resolution Ultrasound Localization Microscopy. *Curr Med Sci.* 2022 Feb.
- [6] Hingot, V., Errico, C., Heiles, B. et al. Microvascular flow dictates the compromise between spatial resolution and acquisition time in Ultrasound Localization Microscopy. *Sci Rep* 9, 2456 (2019).
- [7] Huang, C., Lowerison, M.R., Trzasko, J.D. et al. Short Acquisition Time Super-Resolution Ultrasound Microvessel Imaging via Microbubble Separation. *Sci Rep* 10, 6007 (2020).
- [8] G. Tuccio, L. T. Winkel, C. Bruggeman, W. Van Hoeve and L. Demi, "Increasing Microbubble Concentrations in Microvascular Imaging via Microbubble Separation by means of Orthogonal Frequency Division Multiplexing," 2024 IEEE Ultrasonics, Ferroelectrics, and Frequency Control Joint Symposium (UFFC-JS), Taipei, Taiwan, 2024, pp. 1-4